объединенный
институт
ядерных
исследований
дубна

E2-86-280

D.Yu.Bardin, V.A.Dokuchaeva*

MUON ENERGY SPECTRUM IN INVERSE μ-DECAY

Submitted to "Nuclear Physics"

* Moscow State University, Moscow, USSR

1986

1. Introduction

The inverse μ -decay is one of the simplest purely leptonic processes

$$\nu_\mu e \to \mu^- \nu_e \tag{1}$$

being a cross-channel of the usual μ -decay. Like the latter, it is of great interest for theoretical and experimental physics, because within a renormalizable gauge theory its cross section may be calculated up to a desired accuracy and because the information extracted from the analysis of this process is not affected by strong interaction uncertainties. Therefore, the experimental data are directly related to the underlying properties of the theories.

Within the standard $SU(2)_L \otimes U(1)$ theory /1/ the Born approximation of process (1) is described only by diagram 1 of Fig. 1.

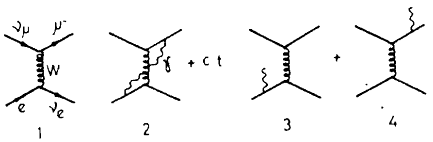

Fig. 1.
Diagrams of the inverse μ -decay process contributing to the QED-part of the cross-section with account of radiative corrections.

The corresponding total cross section neglecting the W-boson propagator effects reads

$$\sigma^B = \frac{G_F^2}{\pi} \frac{(s-m_\mu)^2}{s}, \tag{2}$$

where G_F is the Fermi constant, $m_{e,\mu}$ are the electron and the muon masses, $s = m_e^2 + 2m_e E_\nu$ with E_ν being the incident neutrino energy in the laboratory system.

Reaction (1) has a rather high threshold,

$$E_\nu \gg E_{thr} = \frac{m_\mu^2 - m_e^2}{2m_e} = 10.9\,GeV, \tag{3}$$

which makes it accessible for observation only at the most powerful modern accelerators of CERN and FNAL. About 600 events of reaction (1) were collected in an exposure of the CHARM-I detector[2]. The analysis of the data allows one to set rather strict limits on deviations from V-A interactions, on parameters of a second charged intermediate boson of the $SU(2)_L \otimes SU(2)_R \otimes U(1)$ model, and on an upper limit of the multiplicative lepton number conservation. Much more events will be recorded in CERN CHARM-II experiment which will be ready for exposure in the summer of 86. One can estimate the number of events of reaction (1) from the total cross-section ratio of process (1) and elastic $\nu_\mu e$ scattering, the measurement of which is the main goal of CHARM-II experiment. One has

$$R^{lept}_{NC/CC} = \rho^2\left(\frac{1}{4} - S_\theta^2 + \frac{4}{3}S_\theta^4\right)\Big/\left(1 - m_\mu^2/S\right)^2, \tag{4}$$

where $S_\theta^2 = \sin^2\theta_W$
and

$$\rho = G_F^{NC}/G_F^{CC} = M_W^2/M_Z^2\cos^2\theta_W \tag{5}$$

is another basic parameter of the theory equal to 1 in the standard theory with a minimal Higgs sector.

At $S_\theta^2 = 0.215$[4] ratio (4) equals 1,2,4,8 at E_ν = 15, 20, 30, 100 GeV and 4.7 being averaged over the WBB neutrino spectrum[3]. So, in a planned CHARM-II exposure collecting 2000 $\nu_\mu e$ -elastic events, there will be recorded about 10000events of the inverse μ -decay.

Such a large statistics allows one to obtain rich and various information: to improve essentially all limitations derived in the previous experiment[2], to normalize independently the neutrino flux and, what is more interesting, to realize a proposition of a model-independent determination of ρ with a precision of about 1%. The measurement of ρ in purely leptonic processes is free from systematic theoretical uncertainties unavoidable, for example, in the determination of ρ from the deep-inelastic neutrino cross section ratio $R=\sigma_{NC}/\sigma_{CC}$. The uncertainties are related with an

impossibility to separate, with sufficiently high precision, three types of possible deviations of ρ from unity: proper deviations caused by intrinsic properties of the theory, those induced by higher-order effects (radiative shift) and some unknown effects caused by structure functions or nuclear properties. In the purely leptonic processes the third effects are not present at all, the second ones could be calculated completely, so that proper deviations of ρ could be derived from measurements without any theoretical uncertainty.

The calculation of electroweak radiative corrections to the differential and total cross sections of reaction (1), evidently necessary for realizing any precision measurement, is the main purpose of this paper. As a calculable observable we choose the muon energy spectrum, since the muon lab. energy E_μ is directly measured by a magnetic spectrometer and the angular acceptance of the spectrometer is equal to 100%. Actually, we shall use, instead of E_μ , the dimensionless variable $y = E_\mu/E_\nu$. In view of the expected 1% statistical precision for the total cross section measurement in the CHARM-II detector, the uncertainty of a theoretical analysis should be lesser, say 0.1-0.2% . Obviously, for such a high accuracy one should calculate cross sections at least up to one-loop corrections. The sufficiency of the one-loop approximation will be understood upon analysing the obtained results.

We have already presented an expression for the muon energy spectrum in process (1) with account of one-loop corrections[5]. Those results were derived, however, under two unrealistic assumptions. Firstly, we used an extreme relativistic approximation $S \gg m_\mu^2$ that is obviously incorrect at energies not too far from E_{thr} , eq. (3). Secondly, the formulae have been derived by assuming that events with inner bremsstrahlung photons

$$\nu_\mu e \to \mu \nu_e \gamma \tag{6}$$

are not distinguished experimentally from the radiationless events of process (1) (inclusive with respect to the muon experimental conditions).

In this paper we improve the results of ref.[5] just along these two lines. Here we successively retain m_μ^2 as compared to S, so the resulting expressions are valid up to threshold neutrino energies. A comparison of two calculations shows that the account of a nonvanishing muon mass is important to guarantee the required accuracy of calculations up to E_ν = 100 GeV. In this paper we study also the influence of the bremsstrahlung photon registration threshold on the differential cross section. Let us explain this point in greater detail. If the trigger of an experiment discriminates, for some reasons (for example, due to background conditions), events of process (6) with a lab. photon energy E_γ greater than some threshold value $\bar{E}_\gamma$, then the differential cross section $d\sigma_{all}$ calculated for inclusive conditions is no longer adequate to the experiment observable. From the $d\sigma_{all}$ one should subtract a cross section $d\sigma_{brem}|_{\omega>\bar{\omega}}$ $(\omega = E_\gamma/E_\nu)$ corresponding to the contribution of discriminated events with an inner bremsstrahlung photon. So, observable is the difference

$$\frac{d\sigma_{exp}}{dy} = \frac{d\sigma_{all}}{dy} - \frac{d\sigma_{brem}}{dy}\bigg|_{\omega>\bar{\omega}}. \tag{7}$$

In this paper we calculate just both the terms in (7) rather than the difference (7) as a whole. Such an approach has been proposed in an analogous situation in ref.[6]. It possesses the following advantages. Firstly, the cross section $d\sigma_{all}$ corresponding to ideal inclusive experimental conditions has an independent interest as a limiting case ($\bar{\omega} \to \omega_{max}$) of a real situation and may be compared at $m_\mu^2 \ll s$ with the results of previous calculations[5]. Secondly, which is more important, it turns out that to calculate two terms in difference (7) separately is a more easy task than to calculate the difference (7) as a whole.

As for the case of elastic $\nu_\mu e$-scattering[7,8], all the calculations were performed within the Sirlin renormalization framework [9], providing a unique approach to different reactions and the same normalization of all cross sections to the μ - decay Fermi constant $G_F^{(\mu)}$. It is especially convenient for the analysis of relative measurements where a common factor cancels.

Throughout the calculations we used the evident approximations

$$\frac{m_e^2}{s} \leq 2.5\cdot 10^{-5} \ll 1 \tag{8}$$

and

$$\frac{s}{M_{W,Z}^2} \leq 1.6\cdot 10^{-4} \ll 1 \quad \text{for } E_\nu \leq 1\,TeV, \tag{9}$$

which drastically simplify the resulting formulae and are very far

from introducing an error greater than the required accuracy of calculations. The new calculation (not imploying the extreme relativistic approximation) is essentially based on our previous results [5]. Within the approximations (9) the new calculations are required only for QED diagrams with emission of real and virtual photons from external lines, diagrams 2-4 in Fig. 1. The contribution of all other (non-QED) diagrams can be taken from previous papers[5,12].

The paper is organized as follows. In Sections 2 and 3 we present analytic expressions for the first and second terms in eq. (7), respectively. In Section 4 we present the results of numerical computations by formulae derived in Sects. 2 and 3 and a concluding discussion.

2. Analytic expression for the differential muon spectrum $d\sigma_{all}$

Here we present the results of calculation of the differential cross section of the process

$$\nu_\mu(k_1) + e^-(p_1) \longrightarrow \mu^-(k_2) + \nu_e(p_2)\left[+\gamma(p)\right], \tag{10}$$

as a function of the variable y including all one-loop (1ℓ) electroweak corrections. We remind that the quantity $d\sigma_{all}$, corresponding to the inclusive with respect to the muon experimental conditions, was found by integrating over the whole phase-space of the $\nu\gamma$-system. This allows one to use the $\nu\gamma$ rest frame, which simplifies the calculations essentially. The result looks as follows

$$\frac{d\sigma_{all}^{1\ell}}{dy} = 2\sigma_0\left[1 - r + \frac{\alpha}{\pi}F_a(r_e, r, y)\right]. \tag{11}$$

In eq. (11)

$$\sigma_0 = \frac{\left[G_F^{(\mu)}\right]^2 m_e E_\nu}{\pi},$$

$$r_e = \frac{m_e}{2E_\nu},$$

$$r = \frac{m_\mu^2}{2m_e E_\nu}, \tag{12}$$

and y varies within the limits

$$r \approx r_e + r \leq y \leq 1 + r_e + \frac{r r_e}{1+r_e} \approx 1. \qquad (13)$$

The μ -decay Fermi constant is related to the total muon life time by the well-known formula[9]

$$\frac{1}{\tau_\mu} = \frac{\left[G_F^{(\mu)}\right]^2 m_\mu^5}{192\pi^3}\left(1 - 8\frac{m_e^2}{m_\mu^2}\right)\left[1 + \frac{\alpha}{2\pi}\left(\frac{25}{4} - \pi^2\right)\right]. \qquad (14)$$

The derivation of an explicit expression for $F_a(r_e, r, y)$ was carried out with the aid of the algebraic computer system SCHOONSCHIP[10]. The program of analytic manipulations written for this purpose is essentially analogous to the program described in detail in ref.[11] If $G_F^{(\mu)}$ is used for the cross section normalization, then, actually, only QED diagrams 2,3,4 of Fig. 1 contribute to $F_a(r_e, r, y)$. The contribution of all other weak loops is absorbed by $G_F^{(\mu)}$. (The extraction of the QED-part from the gauge dependent diagram 2 of Fig.1 is unique, and it is done as in refs.[7,8,11-13]) In this sense these electroweak corrections may be called the radiative ones, but one should not forget that only complete calculations of all diagrams prove that just the quantity $G_F^{(\mu)}$ naturally appears as a normalization factor. For definiteness, below we shall use the name "radiative corrections".

The function $F_a(r_e, r, y)$ can be written in a rather compact form

$$\begin{aligned} F_a(r_e, r, y) = (1-r)\Big[&\Big(\ln\frac{y^2}{r r_e} - 2\Big)\ln\Big(1 - \frac{r}{y}\Big) + \ln\frac{y}{r}\ln(1-y) \\ &- Li_2(r) + Li_2(y) + Li_2\Big(\frac{r-y}{1-y}\Big) + \frac{3}{2}(1-r)\ln(1-r)\Big] \\ &+ \frac{1}{2}(1+3r)\Big[Li_2\Big(\frac{1-r/y}{1-r}\Big) - Li_2\Big(\frac{y-r}{1-r}\Big) - \ln\frac{y}{r}\ln\frac{y-r}{1-r}\Big] \\ &+ P_1(r,y) - P_2(r,y)\ln r - P_3(r,y)\ln r_e + P_4(r,y)\ln y \\ &+ P_5(r,y)\ln(1-y) + P_6(r,y)\Big(1 - \frac{r}{y}\Big)\ln\Big(1 - \frac{r}{y}\Big), \end{aligned} \qquad (15)$$

where

$$P_i(r,y) = \sum_{K=-3}^{2} C_{iK}(r) y^K$$

are polynomials in y and

$$Li_2(x) = -\int_0^1 \frac{\ln(1-xy)}{y}\,dy. \qquad (16)$$

Polynomial coefficients of $P_i(r,y)$ can be conveniently defined by the Table.

Table. Coefficients C_{iK}

	-3	-2	-1	0	1	2
1	$-\frac{7}{36}r^3$	$\frac{r^2}{12}\left(1+\frac{7}{2}r\right)$	$-\frac{7}{12}r - \frac{1}{2}r^2 - \frac{1}{6}r^3$	$-\frac{47}{36} + \frac{25}{8}r + \frac{3}{8}r^2$	$-\frac{11}{12} - \frac{1}{4}r$	$\frac{1}{24}$
2	0	$\frac{1}{2}r^2$	$\frac{1}{2}r - 2r^2$	$\frac{1}{4} - \frac{3}{4}r + \frac{3}{2}r^2$	$\frac{1}{2}$	0
3	$\frac{1}{6}r^3$	$\frac{r^2}{4}(1-r)$	$r - \frac{1}{2}r^2$	$-\frac{2}{3}$	0	0
4	0	r^2	$r(1-4r)$	$\frac{3}{2}r^2$	1	0
5	$\frac{1}{6}r^3$	$-\frac{r^2}{4}(1+r)$	$\frac{r}{2}(1+3r)$	$-\frac{23}{12} + \frac{9}{4}r - \frac{3}{2}r^2$	$-\frac{1}{2}$	0
6	0	$\frac{1}{6}r^2$	$-\frac{r}{4}\left(\frac{1}{3}+r\right)$	$\frac{5}{4}\left(\frac{1}{3}+r\right)$	$\frac{1}{2}$	0

In the extreme relativistic regime, $s \gg m_\mu^2$, eq. (15) becomes much simpler

$$F_a(\hat{0},\hat{0},y) = \frac{2}{3}\ln r_e - \left[\ln(1-y) - \frac{1}{2}\ln y + \frac{1}{4} + \frac{1}{2}y\right]\ln r + y\ln y$$

$$+\frac{1}{2}\left[Li_2(1) - Li_2(y) - \ln^2\frac{1-y}{y}\right] - \left(\frac{23}{72} + \frac{1}{2}y\right)\ln(1-y) - \frac{47}{36} - \frac{11}{12}y + \frac{1}{24}y^2,$$

where the symbol $\hat{0}$ signifies that the corresponding mass was set equal to zero everywhere except logarithmic-funcion arguments. Eq. (17) coincides analytically with eq. (12) of ref./5/ and leads to the well-known expression for the total cross section in the one-loop approximation at $s \gg m_\mu^2$ /13/

$$\sigma_{tot}^{1l} = 2\sigma_0\left[1 + \frac{\alpha}{\pi}\left(\frac{19}{24} + \frac{2}{3}\ln r_e - \frac{\pi^2}{6}\right)\right]. \qquad (18)$$

So, eqs. (17) and (18) control the correctness of an extreme relativistic approximation of the exact formulae (16), derived for the first time in this paper.

3. Analytic expression for the spectrum $d\sigma_{brem}/dy|_{\omega>\bar{\omega}}$

The second term in eq. (7) was also derived with the aid of another SCHOONSCHIP program realizing a straightforward integration of the modulo matrix element squared of the bremsstrahlung process (6) over all angular variables. Along this way we intensively used the results and methods of ref./14/. As a byproduct, at an intermediate step we derived an expression for the double differential with respect to y and ω cross section which we also present in this paper. With its aid, in principle, it is possible to improve the account of experimental conditions of discriminating events with internal bremsstrahlung photons replacing the second term in difference (7) by

$$\frac{d\sigma_{brem}}{dy} = \int_0^{\omega_{max}} \frac{d^2\sigma_{brem}}{dy\,d\omega}\,\mathcal{E}(E_\gamma)\,d\omega, \qquad (19)$$

where the function $\mathcal{E}(E_\gamma)$ gives the efficiency of photon registration by a detector. Because the explicit form of $\mathcal{E}(E_\gamma)$ is unknown for us, we replace it by the step function here

$$\mathcal{E}(E_\gamma) = \begin{cases} 1 & \text{for } E_\gamma > \bar{E}_\gamma \\ 0 & \text{for } E_\gamma < \bar{E}_\gamma \end{cases} \qquad (20)$$

leading to the second term in difference (7). In conclusion of this section we list expressions for $d^2\sigma_{brem}$ and $d\sigma_{brem}|_{\omega>\bar{\omega}}$. The double differential spectrum reads

$$\frac{d^2\sigma_{brem}}{dy\,d\omega} = 2\sigma_0\frac{\alpha}{\pi}\Bigg\{-\frac{3yr^2}{\omega_y^4}L_\omega + \frac{1}{\omega_y^3}\Big[3r^2 - 3ry + \big(3r^2 + (3r+2r^2)y\big)L_\omega\Big]$$
$$+\frac{1}{\omega_y^2}\left[-\frac{3r^2}{2y} - 2r^2 + \left(\frac{3}{2} + 2r\right)y - \left(r + 3r^2 + \left(\frac{1}{2} + \frac{3}{2}r\right)y\right)L_\omega\right]$$
$$+\frac{1}{\omega_y}\left[-\frac{r^2}{2y^2} - \left(\frac{1}{2} - 2r^2\right)\frac{1}{y} + 1 - \frac{3}{2}r - \frac{1}{2}y - \left(\frac{1}{2} - \frac{5}{2}r\right)L_\omega\right] + \frac{1-r}{\omega_y - r}$$
$$+\frac{1}{\omega}\left[\frac{r^3}{6y^3} + \frac{r^2(1-r)}{4y^2} + \left(r - \frac{1}{2}r^2\right)\frac{1}{y} - \frac{29}{12} + \frac{7}{4}r + (1-r)L_\omega\right]$$
$$+\omega\left(\frac{r^3}{6y^3} - \frac{r^2}{4y^2} + \frac{1}{12}\right) - \frac{r^3}{3y^3} + \frac{r^2}{2}\left(1 + \frac{r}{2}\right)\frac{1}{y^2} - \frac{r^2}{2y} - \frac{1}{6} + \frac{r}{4}\Bigg\}, \qquad (21)$$

with

$$\omega_y = \omega + y, \quad L_\omega = \ln\left(\frac{y}{r}\,\frac{\omega_y - r}{\omega}\right). \qquad (22)$$

It may be easily integrated over ω within kinematical limits under the restriction $\omega \geqslant \bar{\omega} \gg r_e$. The result is

$$\left.\frac{d\sigma_{brem}}{dy}\right|_{\omega>\bar{\omega}} = 2\sigma_0\,\frac{\alpha}{\pi}\,F_b(r,\bar{\omega},y), \qquad (23)$$

$$F_b(r,\bar{\omega},y)=(1-r)\Big[\frac{1}{2}\ln\frac{1-y}{\bar{\omega}}\ln\frac{y^2(y-r)^2}{r^2\bar{\omega}(1-y)}+Li_2\Big(\frac{\bar{\omega}}{r-y}\Big)-Li_2\Big(\frac{1-y}{r-y}\Big)\Big]$$
$$+\Big(\frac{1}{2}-\frac{5}{2}r\Big)\Big[Li_2\Big(\frac{1}{r}\Big)-Li_2\Big(\frac{1}{y}\Big)+Li_2\Big(\frac{\bar{\omega}_y}{y}\Big)-Li_2\Big(\frac{\bar{\omega}_y}{r}\Big)\Big]$$
$$+\Big\{(\bar{\omega}_y-r)\Big[\frac{\bar{\omega}}{\bar{\omega}_y}\Big(\frac{1}{2}-\frac{r}{\bar{\omega}_y}\Big)-\frac{1}{2}\Big]-r^2\Big(\frac{3}{2}-\frac{1}{2\bar{\omega}_y}\Big)\Big\}\Big(\frac{1}{\bar{\omega}_y}-1\Big)\ln\frac{y(\bar{\omega}_y-r)}{r\bar{\omega}}$$
$$+\Big[\frac{r^3}{6y^3}-\frac{r^2(1+r)}{4y^2}+\frac{r(1+3r)}{2y}-\frac{23}{12}+\frac{9}{4}r-\frac{3}{2}r^2-\frac{1}{2}y\Big]\ln\frac{1-y}{\bar{\omega}}$$
$$+\frac{3}{2}(1-r)^2\ln\frac{1-r}{\bar{\omega}_y-r}+\frac{r}{\bar{\omega}_y^2}(\bar{\omega}+r)-\frac{1}{\bar{\omega}_y}\Big[\frac{r^2}{y}+(1+r)(\bar{\omega}+r)\Big]$$
$$+\bar{\omega}^2\Big(-\frac{r^3}{12y^3}+\frac{r^2}{8y^2}-\frac{1}{24}\Big)+\bar{\omega}\Big[\frac{r^3}{3y^3}-\frac{r^2}{2y^2}\Big(1+\frac{r}{2}\Big)+\frac{r^2}{2y} \tag{24}$$
$$+\frac{1}{6}-\frac{r}{4}\Big]-\frac{r^3}{4y^3}+\frac{r^2}{4y^2}\Big(\frac{3}{2}+\frac{5}{3}r\Big)+\frac{r^2}{2y}\Big(\frac{1}{2}-\frac{1}{3}r\Big)$$
$$+\frac{7}{8}+\frac{5}{4}r+\frac{3}{8}r^2-\frac{1}{4}\Big(\frac{11}{3}+r\Big)y+\frac{1}{24}y^2,$$

with
$$\bar{\omega}_y=\bar{\omega}+y.$$

4. Discussion of numerical results, conclusions

Formulae of Sects. 2 and 3 were realized in a FORTRAN program to compute numerically y -spectra and the total cross section.

For illustrations it is convenient to define dimensionless radiative correction factors

$$\delta_a^{ll}(E_\nu,y)=\frac{d\sigma_{all}^{ll}/dy}{d\sigma^B/dy}-1=\frac{\alpha}{\pi}(1-r)^{-1}F_a(r_e,r,y), \tag{25}$$

$$\delta_b(E_\nu,y)=\frac{d\sigma_{brem}/dy}{d\sigma^B/dy}=\frac{\alpha}{\pi}(1-r)^{-1}F_b(r,\bar{\omega},y), \tag{26}$$

$$\delta_a^t(E_\nu)=\frac{\sigma_{all}^{ll}}{\sigma^B}-1=\frac{\alpha}{\pi}(1-r)^{-2}\int_r^1 F_a(r_e,r,y)\,dy, \tag{27}$$

$$\delta_b^t(E_\nu)=\frac{\sigma_{brem}}{\sigma^B}=\frac{\alpha}{\pi}(1-r)^{-2}\int_r^{1-\bar{\omega}} F_b(r,\bar{\omega},y)\,dy. \tag{28}$$

In the extreme relativistic regime (27) becomes

$$\delta_a^t(E_\nu)=\frac{\alpha}{\pi}\Big(\frac{19}{24}-\frac{2}{3}\ln\frac{2E_\nu}{m_e}-\frac{\pi^2}{6}\Big). \tag{29}$$

In Fig. 2 the corrections to the total cross section (27) and (29) are shown for a wide range of incident neutrino energies E_ν from the reactions threshold 10.9 GeV to 1 TeV.

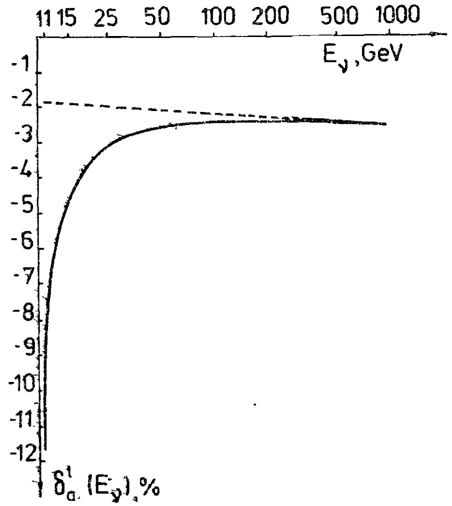

Fig.2.
The radiative correction $\delta_a^t(E_\nu)$ calculated by exact (solid line) and extreme relativistic (dashed line) formulae.

As is seen up to E_ν = 100 GeV, there is a significant difference between exact in m_μ, formula (27), and extreme relativistic eq. (29), calculations. Near the maximal intensity of the CERN neutrino WBB, E_ν^m = 15 GeV, the approximate correction is three times smaller than the exact one, which evidently necessitates the account of nonvanishing m_μ in calculations of radiative corrections.

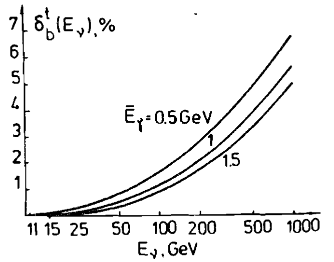

Fig. 3.
The correction $\delta_b^t(E_\nu)$ calculated at different $\bar{E}_\gamma$ values. The numbers near the curves are incident neutrino energies in GeV.

In Fig. 3 the correction (28) is shown for the same energy range and at $\bar{E}_\gamma$ = 0.5, 1.0 and 1.5 GeV. As is seen, the quantity $\delta_b^t(E_\nu)$ increases with increasing E_ν and decreasing $\bar{E}_\gamma$. The corrections averaged over the WBB-spectrum are

$$\langle \delta_a^t(E_\nu) \rangle = -2.7\%,$$
$$\langle \delta_b^t(E_\nu) \rangle = 1.0\% \text{ at } \bar{E}_\gamma = 0.5 \text{ GeV}. \tag{30}$$

So, the resulting radiative correction to the process (10) under the conditions of CHARM-II experiment is -3.7% that is much greater than the proposed statistical errors in the measurement of the total cross section ($\Delta\sigma/\sigma \simeq 1\%$) - and parameter ρ ($\Delta\rho/\rho \simeq 1\%$).

From the above analysis we draw the main conclusion of this paper: radiative corrections to the inverse μ-decay are rather large in the above sense, and their calculations should be done by using formulae exact in m_μ, i.e., avoiding the approximation $m_\mu^2 \ll S$ and taking into account the threshold of discrimination of events with bremsstrahlung photons, $\bar{E}_\gamma$. The neglect

of these corrections in the data processing will lead, for example, to a systematic error in the determination of ρ higher than the statistical error in the measurement of ρ.

To obtain a more detailed information about radiative corrections, in particular, about the accuracy level of the performed calculations, let us analyse the corrections (25) and (26) differential with respect to y.

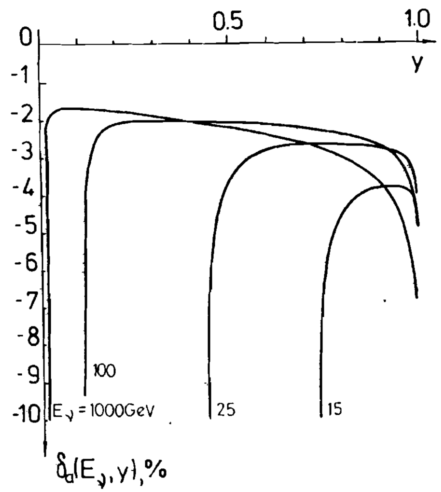

Fig. 4.
Radiative corrections $\delta_a^{te}(E_\nu, y)$ at different initial neutrino energies E_ν as functions of the variable y. The numbers near the curves are values of E_ν in GeV.

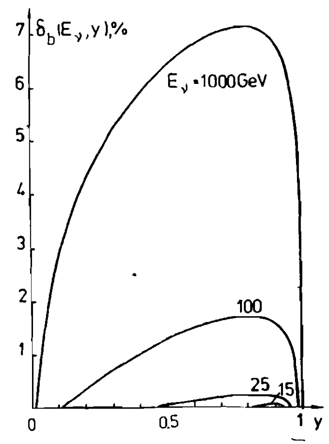

Fig. 5.
The corrections $\delta_b(E_\nu, y)$ at different initial neutrino energies E_ν and at $\bar{E}_\gamma$ = 1 GeV, as a function of the variable y. The numbers near the curves are values of E_ν in GeV.

In Figs. 4 and 5 corrections $\delta_a^{ll}(E_\nu, y)$ and $\delta_\ell(E_\nu, y)$ at $\bar{E}_\gamma$ = 1 GeV are shown for four incident neutrino energies E_ν = 15, 25, 100 and 1000 GeV. Due to corrections the y -distribution flat in the Born approximation is distorted. Near the kinematical boundaries $y_{min} = r$ and y_{max} = 1 the correction δ_a^{ll} becomes negative and large. In both cases this is the usual infrared behaviour. The minus-infinity trend of the correction is due to the kinematic possibility of emission of only very soft photons in definite phase space subregions. There the large positive contribution of hard photons is suppressed. So, when $y \to 1$, the energy is carried away by the muon, and the phase space available to the $\nu\gamma$ -system becomes very small. When $y \to y_{min}$, from the analysis of kinematics one may conclude that the neutrino tries to carry the energy $E_\nu - E_\mu$, and again the photon phase space vanishes. In the infrared regions the contributions of higher perturbative orders are not small. The summation procedure known as exponentiation is justified here, namely, the replacement

$$1 + \delta_a^{ll}(E_\nu, y) \Rightarrow e^{\delta_a^{ll}(E_\nu, y)} \qquad (31)$$

takes, with a high precision, account of higher order terms.

If the replacement (31) is continued over the whole region of y, we shall make an error, but due to the smallness of δ_a^{ll} at intermediate y the introduced error is lower than the required accuracy of calculations, 0.1%. The other term, $\delta_\ell(E_\nu, y)$, is sufficiently small by itself ($< 3\%$ for $E_\nu \leq$ 200 GeV), hence the error $\Delta\delta_\ell$ caused by the neglect of terms of higher order in α is also of an order of one tenth of per cent. So, the expression

$$\frac{d\sigma}{dy} = 2\sigma_0 (1-r)\left[e^{\delta_a^{ll}(E_\nu, y)} - \delta_\ell(E_\nu, y)\right] \qquad (32)$$

ensures the claimed accuracy of calculations of an order of 0.1 - 0.2%. We note that as a result of the exponentiation, the y -distribution changes its flat shape to a bell-like shape going fast to zero in narrow vicinities of kinematic boundaries. As follows from Fig.5, $d\sigma_{Brem}$ already possesses this property.

The vanishing of $d\sigma_{all}^{ll}$ is a consequence of the replacement (31) taking into account that $\delta_a^{ll} \to -\infty$ as $y \to y_{min,\,max}$. As an example, we presented in Fig. 6 the differential distribution $(2\sigma_0)^{-1} d\sigma/dy$ at two values of E_ν and $\bar{E}_\gamma$ = 1 GeV. The deviation from the flat shape is visibly small, and whether it will be noticed in future experiments or not depends on concrete experimental conditions, in particular, on $\langle E_\nu \rangle$ and $\bar{E}_\gamma$.

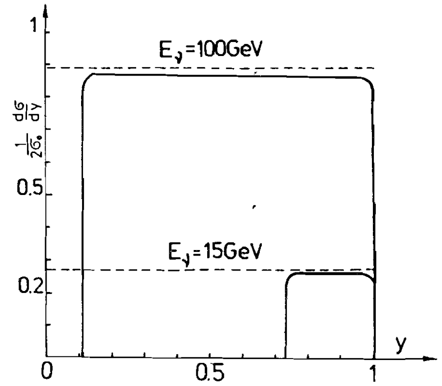

Fig. 6.
The muon energy spectrum in the inverse μ -decay at two initial neutrino energies calculated with (solid lines) and without (dashed lines) radiative corrections.

In any case the set of formulae presented here together with formulae of refs. /7,8/ for elastic $\nu_\mu e$ -scattering allows one to perform, with a sufficiently high accuracy, the procedure of radiative corrections in the analysis of the future precision data of CHARM-II experiment on the inverse μ -decay and elastic $\nu_\mu e$ -scattering.

The authors are very much obliged to K.Winter for raising this problem and also to A.A.Akhundov, T.Riemann and A.N. Rosanov for fruitful discussions and critical comments in reading the manuscript.

References

1. S.L.Glashow, Nucl.Phys. 22 (1961) 579;
S.Weinberg, Phys.Rev. Lett. 19 (1967) 1263;
A. Salam, Elementary Particle Theory (ed. N.Svartholm) (Almqvist and Wiksell, Stockholm, 1968), p. 367.
2. F.Bergsma et al., Phys. Lett. 122B (1983) 465.

3. C.Busi et al., CERN /SPSC/83-24, CERN/SPSC/83-37 (1983).
4. F.Bergsma et al., Phys.Lett. 147B (1984) 481.
5. D.Yu.Bardin and V.A.Dokuchaeva, JINR Comm. E2-86-260 (1986).
6. D.Yu.Bardin and V.A.Dokuchaeva, Yad. Fiz. 39 (1984) 888.
7. S.Sarantakos, A.Sirlin and W.J.Marciano, Nucl. Phys. B217 (1983) 84.
8. D.Yu.Bardin and V.A.Dokuchaeva, Nucl. Phys. B246 (1984) 221.
9. A.Sirlin, Phys.Rev. D22 (1980) 971.
10. H.S.Strubbe, Comp. Phys. Com. 8 (1974) 1.
11. D.Yu.Bardin and V.A.Dokuchaeva Yad.Fiz. 43 (1986) 1513.
12. D.Yu.Bardin, P.Ch. Christova and O.L.Fedorenko, Nucl.Phys. B197 (1982) 1.
13. A.Sirlin and W.J.Marciano, Nucl. Phys. B189 (1981) 442.
14. A.A.Akhundov and D.Yu.Bardin, JINR Comm. P2-9587 (1976).
15. D.Yennie, S.Frautschi and H.Suura, Ann. Phys. 13 (1961) 379.

Received by Publishing Department
on April 29, 1986.

Бардин Д.Ю., Докучаева В.А. E2-86-280

Энергетический спектр мюонов в процессе обратного μ-распада

Вычислен энергетический спектр мюонов в процессе обратного μ-распада. Расчет выполненен с точностью до однопетлевых электрослабых поправок без пренебрежения массой мюона и с учетом порога регистрации фотонов внутреннего тормозного излучения. Показано, что в условиях эксперимента CHARM-II /ЦЕРН/ суммарная поправка к полному сечению составляет-4%.

Работа выполнена в Лаборатории теоретической физики ОИЯИ.

Препринт Объединенного института ядерных исследований. Дубна 1986

Bardin D.Yu., Dokuchaeva V.A. E2-86-280

Muon Energy Spectrum in Inverse μ-Decay

The muon energy spectrum for the inverse μ-decay is calculated up to one-loop electroweak corrections, avoiding the neglect of the muon mass and taking into account the registration threshold of inner bremsstrahlung photons. It is shown that under the conditions of new CHARM-II experiment at CERN the overall correction to the total cross-section approaches -4%.

The investigation has been performed at the Laboratory of Theoretical Physics, JINR.

Preprint of the Joint Institute for Nuclear Research. Dubna 1986